ARMY RESEARCH LABORATORY

Moments on a Coning M864 by a Liquid Payload: The Candlestick Problem and Porous Media

by Gene R. Cooper

ARL-TR-3837 **July 2006**

Approved for public release; distribution is unlimited.

NOTICES

Disclaimers

The findings in this report are not to be construed as an official Department of the Army position unless so designated by other authorized documents.

Citation of manufacturer's or trade names does not constitute an official endorsement or approval of the use thereof.

DESTRUCTION NOTICE—Destroy this report when it is no longer needed. Do not return it to the originator.

Army Research Laboratory
Aberdeen Proving Ground, MD 21005-5066

ARL-TR-3837 **July 2006**

Moments on a Coning M864 by a Liquid Payload: The Candlestick Problem and Porous Media

Gene R. Cooper
Weapons and Materials Research Directorate, ARL

Approved for public release; distribution is unlimited.

REPORT DOCUMENTATION PAGE

Form Approved
OMB No. 0704-0188

Public reporting burden for this collection of information is estimated to average 1 hour per response, including the time for reviewing instructions, searching existing data sources, gathering and maintaining the data needed, and completing and reviewing the collection information. Send comments regarding this burden estimate or any other aspect of this collection of information, including suggestions for reducing the burden, to Department of Defense, Washington Headquarters Services, Directorate for Information Operations and Reports (0704-0188), 1215 Jefferson Davis Highway, Suite 1204, Arlington, VA 22202-4302. Respondents should be aware that notwithstanding any other provision of law, no person shall be subject to any penalty for failing to comply with a collection of information if it does not display a currently valid OMB control number.
PLEASE DO NOT RETURN YOUR FORM TO THE ABOVE ADDRESS.

1. REPORT DATE *(DD-MM-YYYY)*	2. REPORT TYPE	3. DATES COVERED (From - To)
July 2006	Final	May 2004 to December 2004

4. TITLE AND SUBTITLE

Moments on a Coning M864 by a Liquid Payload: The Candlestick Problem and Porous Media

5a. CONTRACT NUMBER

5b. GRANT NUMBER

5c. PROGRAM ELEMENT NUMBER

6. AUTHOR(S)

Gene R. Cooper (ARL)

5d. PROJECT NUMBER
622618.H8099

5e. TASK NUMBER

5f. WORK UNIT NUMBER

7. PERFORMING ORGANIZATION NAME(S) AND ADDRESS(ES)
U.S. Army Research Laboratory
Weapons and Materials Research Directorate
Aberdeen Proving Ground, MD 21005-5069

8. PERFORMING ORGANIZATION REPORT NUMBER
ARL-TR-3837

9. SPONSORING/MONITORING AGENCY NAME(S) AND ADDRESS(ES)

10. SPONSOR/MONITOR'S ACRONYM(S)

11. SPONSOR/MONITOR'S REPORT NUMBER(S)

12. DISTRIBUTION/AVAILABILITY STATEMENT

Approved for public release; distribution is unlimited.

13. SUPPLEMENTARY NOTES

14. ABSTRACT

Moments that are caused by a payload assumed to be an inviscid liquid flowing in a coning projectile are predicted. This payload is contained in a uniform sequence of end-to-end cylinders stacked in columns along and off the symmetry axis of the projectile. A theoretical model is used to analyze inertial waves passing through the liquid, which are generated by the coning motion. This analysis continues by considering a single column along the projectile symmetry axis, which is filled with an inviscid fluid saturating porous media. Eigen frequencies and their impact on liquid moments are discussed concerning the flight stability of the projectile for a wide range of payload configurations and porosities when the projectile is subjected to various coning frequencies.

15. SUBJECT TERMS

16. SECURITY CLASSIFICATION OF:			17. LIMITATION OF ABSTRACT	18. NUMBER OF PAGES	19a. NAME OF RESPONSIBLE PERSON
a. REPORT	b. ABSTRACT	c. THIS PAGE			Gene R. Cooper
Unclassified	Unclassified	Unclassified	SAR	25	19b. TELEPHONE NUMBER (*Include area code*) 410-278-3684

Standard Form 298 (Rev. 8/98)
Prescribed by ANSI Std. Z39.18

Contents

List of Figures

Acknowledgments

The author wishes to acknowledge Kok Y. Chung, of the U.S. Army Research, Development, and Engineering Center (ARDEC), for his guidance, suggestions and technical assistance which had a great impact on this work. Mr. Chung kept the author informed of new design and geometric configurations, thus causing the investigation to closely address the Army concerns regarding liquid non-lethal payloads. This work was funded by ARDEC.

INTENTIONALLY LEFT BLANK.

1. Introduction

Predicting the moment attributable to a liquid payload in a spinning and coning projectile is a problem of considerable interest to the Army. Stewartson (*1*) was first to consider inviscid payloads contained in a right circular cylinder, and his results gave coning Eigen frequencies that can possibly cause catastrophic yaw for a liquid-carrying projectile. First order viscous boundary layer corrections of the Stewartson theory were made by Wedemeyer (*2*) and Murphy (*3*). A method for calculating the linear liquid moment using the full linear viscous equations with boundary layer corrections confined only to the end caps (candlesticks) was presented by Hall, Sedney, and Gerber (*4, 5*).

A further interest to the army is to consider a series of uniform circular cylinders stacked end to end separated by impenetrable end caps. These candlesticks may be situated along the symmetry axis or offset from this axis but parallel to the symmetry axis of the projectile. Coning motion-induced liquid moments are considered here for a number of candlestick configurations. The Eigen frequencies for such configurations are shown to be identical to those found by Stewartson (*1*).

Liquid payloads contained in a highly permeable material have been of interest to the U.S. Army for some time. Laboratory tests and flight tests have shown that a highly permeable medium can significantly reduce the spin-up time of a liquid payload (*6, 7, 8*). Flight stability for liquid-saturated permeable payloads has also been examined by D'Amico (*9, 10*). An investigation by Cooper (*11*) considered inertial waves in a coning projectile with a saturated porous media payload so that the media are homogenous and isotropic. The present work extends the Stewartson and Cooper problems by considering a cylindrical cavity filled with a permeable medium that is impregnated with an inviscid liquid, but this medium is not necessarily isotropic. Following Cooper, we introduced a further modification by segmenting the cavity along the symmetry axes into a sequence of equal length cylinders. Each of these cylinders is separated by impermeable end caps. The porous media are modeled by a drag term, which is proportional to the liquid velocity relative to the assumed ridge porous media that are added to the linearized Euler equations. This analysis examines the induced liquid moment as a function of parameters found by Stewartson (*1*) plus parameters describing the porous media and the number of segments in the cylindrical cavity.

2. Equations of Motion for the Off-Axis Candlestick Configurations

Figure 1 shows the X', Y', Z' axes rotating uniformly about X' with angular velocity $\mathbf{P} = (P,\ 0,\ 0)$, and figure 2 presents details of the internal configuration of the candlestick payloads. The liquid is

assumed to be initially rotating as a rigid body with the same angular speed $\mathbf{P}$ so the velocity $\mathbf{V}'$ of the liquid inside the cylinders is

$$\mathbf{V}' = \mathbf{P} \times \left(x,\ \ R_0 \cos B + r\cos\theta,\ \ R_0 \sin B + r\sin\theta\right) \tag{1}$$

The unperturbed state for equation 1 satisfies the Euler equation:

$$P^2\ \mathbf{e}_x \times \left(\mathbf{e}_x \times \left(x,\ \ R_0 \cos B + r\cos\theta,\ \ R_0 \sin B + r\sin\theta\right)\right) = -\nabla \frac{P_s}{\rho} \tag{2}$$

for which P_s is the unperturbed liquid pressure. Following Stewartson and letting the position vector have the Cartesian form $\mathbf{R} = \left(x,\ \ R_0 \cos B + r\cos\theta,\ \ R_0 \sin B + r\sin\theta\right)$ allows equation 2 to be integrated as a scalar potential so that

$$P_S/\rho = P^2 R_0 \cos\left(B - \theta\right) - P^2 r^2/2 \tag{3}$$

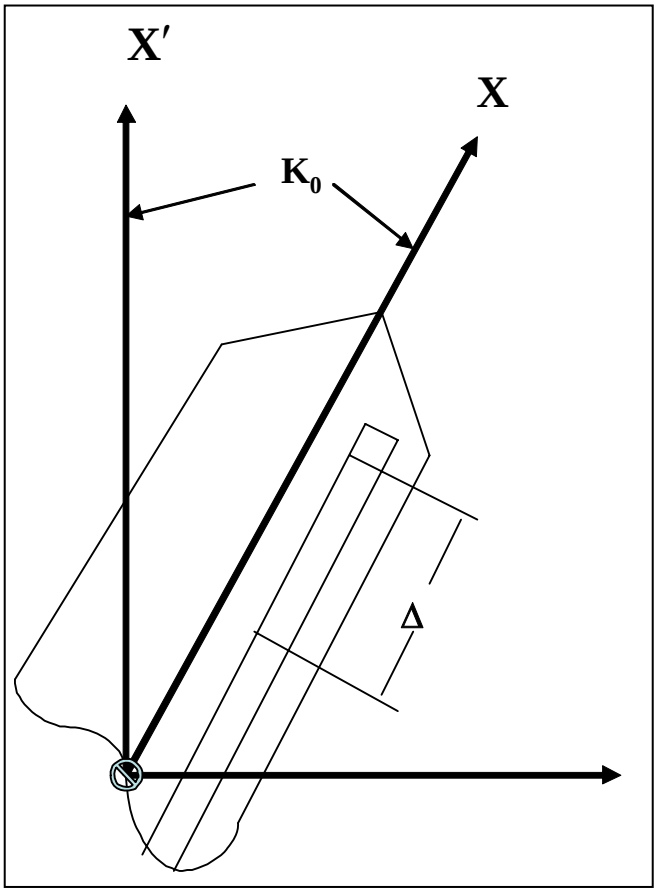

Figure 1. Coordinate systems of configuration.

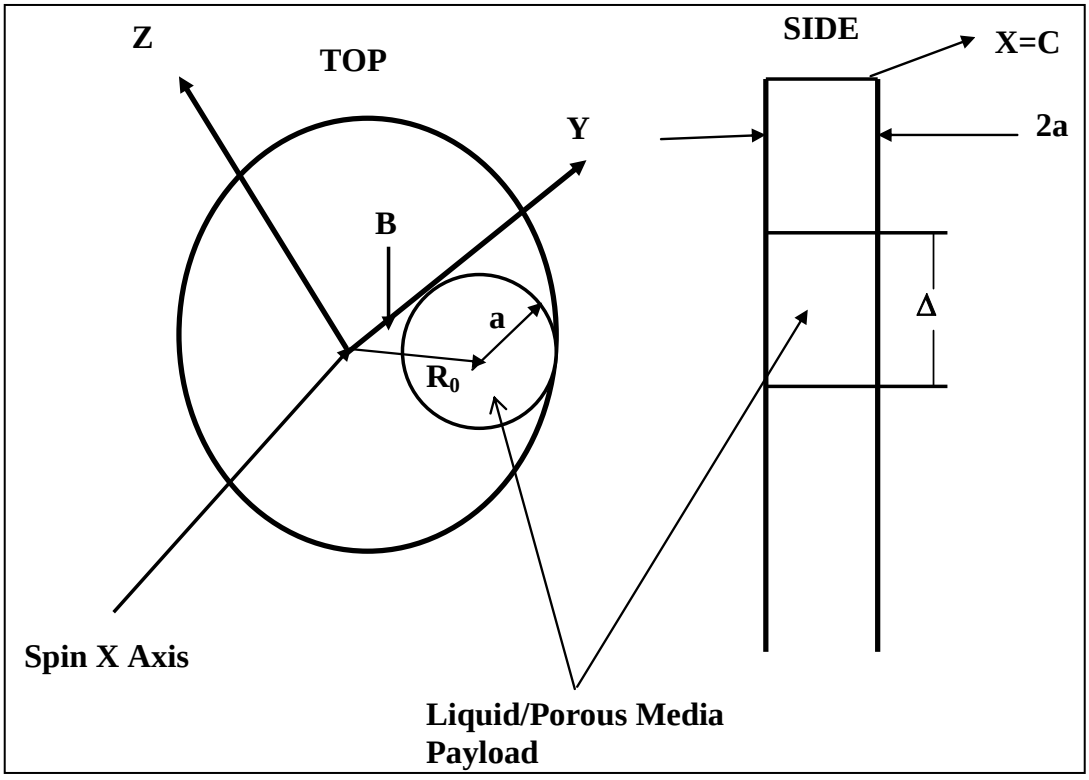

Figure 2. Details of payload configuration.

Now we excite wave motion in the rigidly rotating liquid by perturbing the angular velocity of the projectile for small angular components, ω_y, ω_z, so that the total angular velocity takes the form

$$\mathbf{\Omega} = \mathbf{P} + (0,\ \omega_y,\ \omega_z). \tag{4}$$

The projectile is assumed to undergo small angle coning motion about the X', Y', Z' frame and is related to the projectile body axes, X, Y, Z, by the following transformation (*3*):

$$\begin{bmatrix} X' \\ Y' \\ Z' \end{bmatrix} = \begin{bmatrix} 1 & 0 & 0 \\ 0 & \cos[tPT] & -\sin[PT] \\ 0 & \sin[tPT] & \cos[tPT] \end{bmatrix} \begin{bmatrix} 1 & -K_0 e^{\varepsilon TPt} & 0 \\ K_0 e^{\varepsilon TPt} & 1 & 0 \\ 0 & 0 & 1 \end{bmatrix} \begin{bmatrix} 1 & 0 & 0 \\ 0 & \cos[tP(T-1)] & \sin[tP(T-1)] \\ 0 & -\sin[tP(T-1)] & \cos[tP(T-1)] \end{bmatrix} \begin{bmatrix} X \\ Y \\ Z \end{bmatrix} \tag{5}$$

where the coning damping rate is ε the coning frequency is T and K_0 is the magnitude of the small coning angle. Equation 5 shows that the angular velocity, to first order in K_0, is written as a column vector with body frame components

$$\begin{bmatrix} P \\ -K0\,P\,T\left[\varepsilon\sin(tP(T-1)) + \cos(tP(T-1))\right]e^{\varepsilon PTt} \\ -K0\,P\,T\left[\sin(tP(T-1)) - \varepsilon\cos(tP(T-1))\right]e^{\varepsilon PTt} \end{bmatrix} \tag{6}$$

This suggests that the velocity of the liquid payload should be given by

$$\mathbf{V} = \mathbf{P} \times \left(x,\ \ R_0 \cos B + r \cos\theta,\ \ R_0 \sin B + r \sin\theta \right) + \hat{\mathbf{v}} \tag{7}$$

for which the components of $\hat{\mathbf{v}}$ and the pressure perturbation $\hat{p}$ all have the magnitudes of order K_0.

The liquid payload is assumed to have low viscosity and the magnitude P is assumed to be large so that the fluid motion is adequately described by Euler's equations. (The M864 projectile in free flight with a water payload has a Reynolds number on the order of 10^6.) Neglecting all higher order terms in small K_0 makes the Euler equations take the following form:

$$\begin{aligned} \frac{d\hat{V}}{dt} - 2P\hat{W} + \frac{1}{\rho}\frac{d\hat{p}}{dr} &= 0 \\ \frac{d\hat{W}}{dt} + 2P\hat{V} + \frac{1}{\rho r}\frac{d\hat{p}}{d\theta} &= 0 \\ \frac{d\hat{U}}{dt} \qquad\qquad + \frac{1}{\rho}\frac{d\hat{p}}{dx} &= 0 \end{aligned} \tag{8}$$

in which $\left(\hat{V},\ \ \hat{W},\ \ \hat{U} \right)$ are cylindrical components of the perturbed velocity for the perturbed pressure, $\hat{p}$.

Normal boundary conditions at the solid wall satisfy

$$\left(\hat{V},\ \ \hat{W},\ \ \hat{U} \right) \bullet \mathbf{n} = \boldsymbol{\Omega} \times \mathbf{Rs} \bullet \mathbf{n} \tag{9}$$

in which $\mathbf{n}$ is an outward unit vector on the wall and $\mathbf{Rs}$ a point on any cylinder wall. Equation 6 when substituted into equation 9 causes the normal boundary conditions to become

$$\begin{aligned} \hat{V} &= \Re e\left(x\, K_0\, P\, S\, e^{PSt - iPt - i\theta} \right) \\ \hat{U} &= -\Re e\left(K_0\, P \left(e^{iB} R_0 + r\, e^{i\theta} \right) S\, e^{PSt - iPt - i\theta} \right). \\ i &= \sqrt{-1},\ S \equiv (\varepsilon + i)T \end{aligned} \tag{10}$$

These show that separable solutions to equation 8 are obtained by

$$\begin{bmatrix} \hat{V} \\ \hat{W} \\ \hat{U} \\ \hat{p} \end{bmatrix} = \begin{bmatrix} v \\ w \\ u \\ p \end{bmatrix} e^{PSt - iPT - i\theta} \tag{11}$$

and solving for the velocity components yields

$$
\begin{aligned}
v &= -\frac{\frac{dp}{dr} r (S-i) + 2\frac{dp}{d\theta}}{r\rho P (S-3i)(S+i)} \\
w &= -\frac{\frac{dp}{d\theta}(S-i) - 2r\frac{dp}{dr}}{r\rho P (S-3i)(S+i)} \\
u &= -\frac{\frac{dp}{dx}}{\rho P (S-i)}
\end{aligned}
\tag{12}
$$

Using the continuity equation, $\nabla \bullet (v,\ w,\ u) = 0$, produces the following equation for the pressure p:

$$
\begin{aligned}
& r^2 \frac{d^2 p}{dr^2} + r\frac{dp}{dr} + \frac{d^2 p}{d\theta^2} - r^2 \sigma^2 \frac{d^2 p}{dx^2} = 0 \\
& \sigma^2 = -\frac{(S-3i)(S+i)}{(S-i)^2}
\end{aligned}
\tag{13}
$$

At this point in the analysis, it is useful to consider each cylindrical candlestick ranging from $-C \le x \le C$ to consist of an end-to-end sequence of N equal length, Δ, cylinders with impenetrable end caps so that $\Delta = 2C/N$. Applying equation 10 to each of the sub-cylinders gives the following Fourier-Bessel series for the pressure in the given candlestick:

$$
\begin{aligned}
p &= K_0 P^2 a^2 \rho \left[\begin{array}{l} e^{-i\theta} \sum_{k \in odd} A_k \cos(\pi k (C+x)/\Delta) J_1(\pi k \sigma r/\Delta) \\ + (r x E/a^2 + r D/a) e^{i\theta} + F x \end{array} \right] \\
A_k &= -\frac{16(-1)^n C S^2 (S-3i)}{\pi^2 a k N (J_1(zz)(S+i) - zz J_0(zz)(S-i))} \\
zz &= \pi a k \sigma N/2C \\
E &= (S-i)S \\
D &= 2C(N-2n-1)S^2/Na \\
F &= e^{iB} R_0 (S-i)S/a \\
0 &\le n \le N,
\end{aligned}
\tag{14}
$$

3. Candlestick(s) Liquid Moments

The moment induced by the liquid contained in the segmented cavity is calculated from the time derivative of the angular momentum field. Non-dimensionalizing the moment with $2\pi\rho a^4 C P^2$ makes it convenient to write the side moment components, M_Y, M_Z, as (*3*):

$$
\begin{aligned}
&M_Y\,\mathbf{J} + M_Z\,\mathbf{K} = T\mathbf{C_{LM}}\left(2\pi\rho a^4 C P^2\right)K_0\, e^{PSt - iPt} \\
&C_{LM} = C_{LSM}(T, N, C)\mathbf{J} + C_{LIM}(T, N, C)\mathbf{K}
\end{aligned}
\tag{15}
$$

Therefore, the induced moment on the entire candlestick consisting of N end-to-end sub-cylinders of length Δ is given by

$$
T\mathbf{C_{LM}}\left(2\pi\rho a^4 C P^2\right) = -\sum_{n=0}^{N-1}\Re\left\{\int \mathbf{R}\times\left[\begin{array}{l}\left(\dfrac{d\hat{V}}{dt} - 2P\hat{W}\right)\mathbf{e_r} + \\ \left(\dfrac{d\hat{W}}{dt} + 2P\hat{V}\right)\mathbf{e_\theta} + \\ \dfrac{d\hat{U}}{dt}\mathbf{e_x}\end{array}\right] d\Omega\right\}
\tag{16}
$$

$$\Omega = 2\pi a^2 \Delta$$

Note that symmetry attributable to the geometry of each candlestick and equation 14 causes the axial component of $\mathbf{C_{LM}}$ to integrate identically to zero.

The calculation of equation 16 is tedious. The details are not given here (*3, 11*), but the result is the following expression:

$$
\begin{aligned}
T(M_Y + i\,M_Z) = &\frac{iS\left(\begin{array}{l}\left(12\cos B\, e^{iB} N^2 R_0{}^2 + i\left(4C^2 + 3a^2\right)N^2 - 8iC^2\right)S \\ -12i\cos B\, e^{iB} N^2 R_0{}^2 - \left(4C^2 - 3a^2\right)N^2\end{array}\right)}{12a^2 N^2} + \frac{2C^2 S^2 (S - i)}{3a^2 N^2 (S + i)} + \\
&\frac{128 C^2 S^3 (S - 3i)}{\pi^4 a^2 N^2 (S + i)} \sum_{k\in odd} \frac{J_1(zz)}{\left[J_1(zz)(S + i) - zz\, J_0(zz)(S - i)\right]k^4}
\end{aligned}
\tag{17}
$$

$$zz = \pi a k \sigma N / 2C,$$

The summation terms of equation 17 show that large over-turning moments can result if

$$
\begin{aligned}
&J_1(zz)(S + i) - zz\, J_0(zz)(S - i) = 0 \\
&zz = \pi a k \sigma N / 2C, k \in \text{odd}
\end{aligned}
\tag{18}
$$

This is the same criterion first found by Stewartson (*1*) for the symmetrically located liquid payload, i.e., at $R = 0$. This says that the Stewartson tables can be used to determine such Eigen frequencies where the aspect ratio is taken to be $2C/a\,N$.

One further comment regarding equation 17 is that $\mathbf{C_{LM}}$ approaches the value produced by a frozen liquid as N becomes large, provided that Eigen frequencies are sufficiently removed from the region of interest. In fact, the rate of approach to the frozen limit is very rapid since it goes as $1/N^2$. Typical coning frequencies of the M864 are presented in figure 3. Figures 3 and 4

give examples of moment coefficients, C_{LSM}, C_{LIM}, for the M864 projectile. The value for the axes' offset is taken to be $R = 2a$ and the orientation angle is $B = \pi/3$. In these plots, the sharp spikes correspond to the increased over-turning moment, C_{LSM}, that is encountered when the projectile's coning frequency passes a Stewartson Eigen frequency. These results clearly show that even for small values of N, the moment coefficients are very close to the frozen limit values. The reason for this is the aspect ratio for these examples is relatively large. Some mathematical manipulations of equation 17 show that for large aspect ratios, the values C_{LSM}, C_{LIM} approach their frozen limit values for all values of N as long as equation 18 is not satisfied. Figure 3 shows that coning rates are in the range of $0 \le T \le 0.1$, and figures 4 and 5 indicate that large over-turning moments caused by the liquid payload should not result in flight instabilities for the parameters examined here. However, if the parameters and particularly, the aspect ratio, were to change, instabilities could result (see figure 6 as an example).

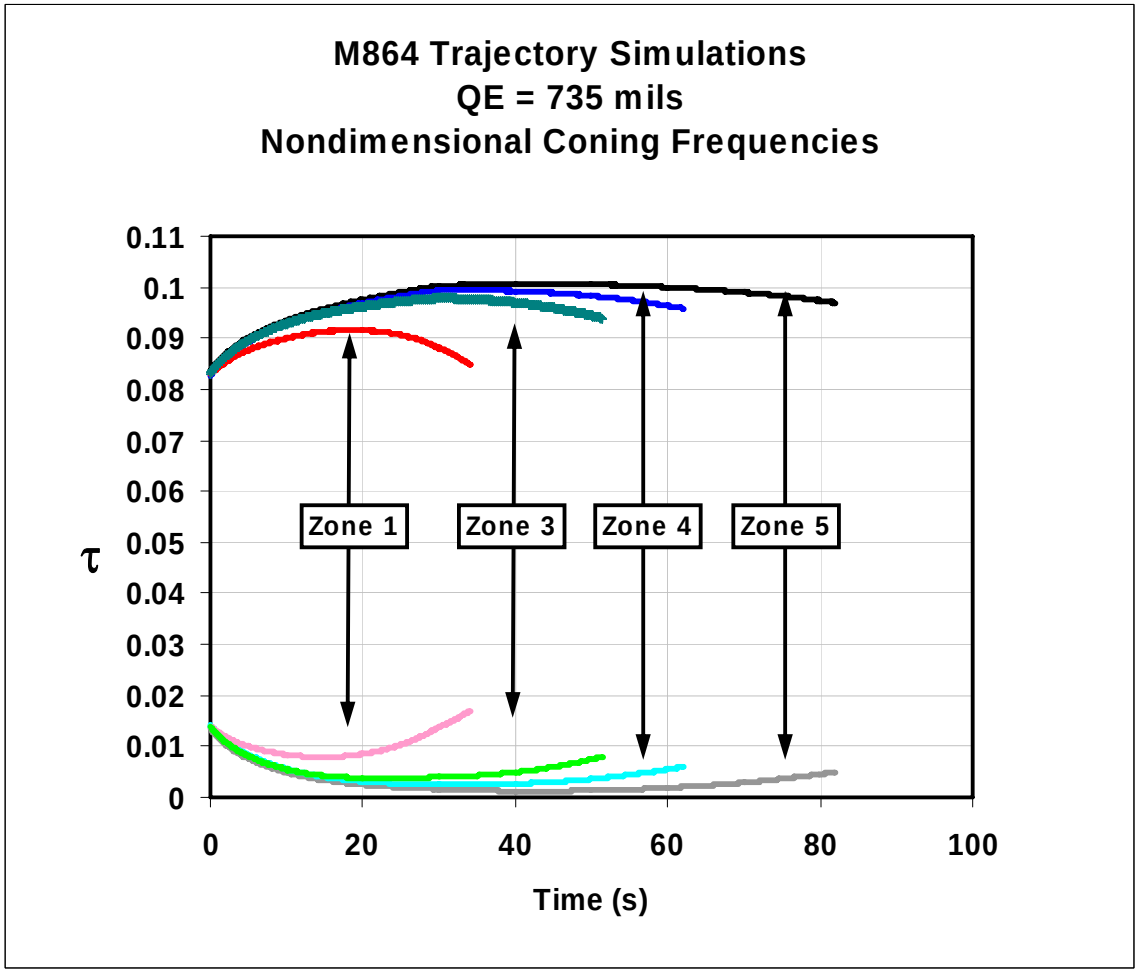

Figure 3. Free flight coning frequencies of the M864 projectile.

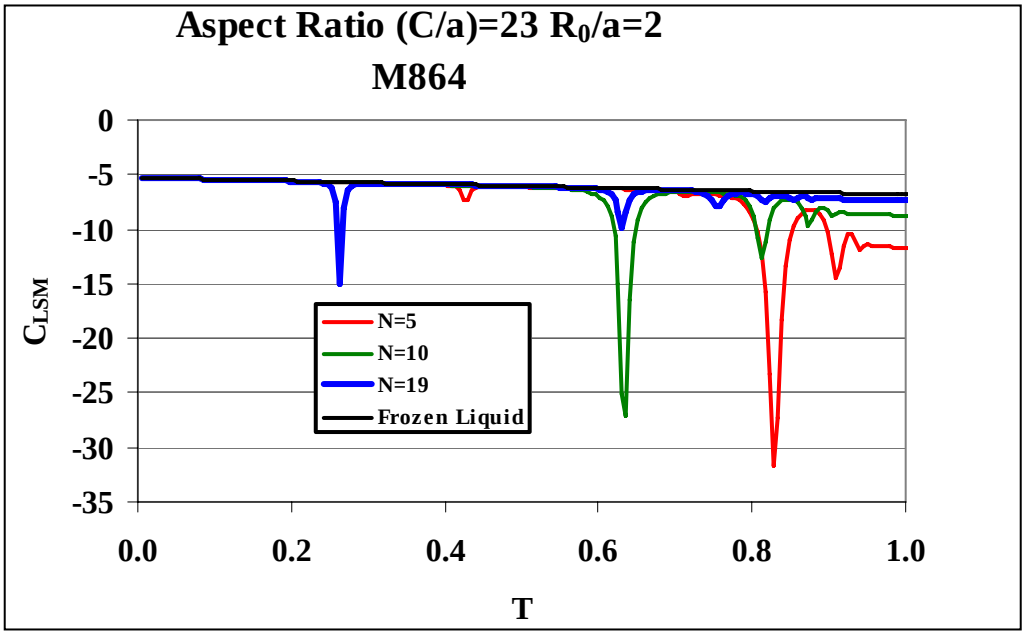

Figure 4. Values of $\mathbf{C_{LSM}}$ showing Eigen frequencies as a function of $\mathbf{T}$ and $\mathbf{N}$.

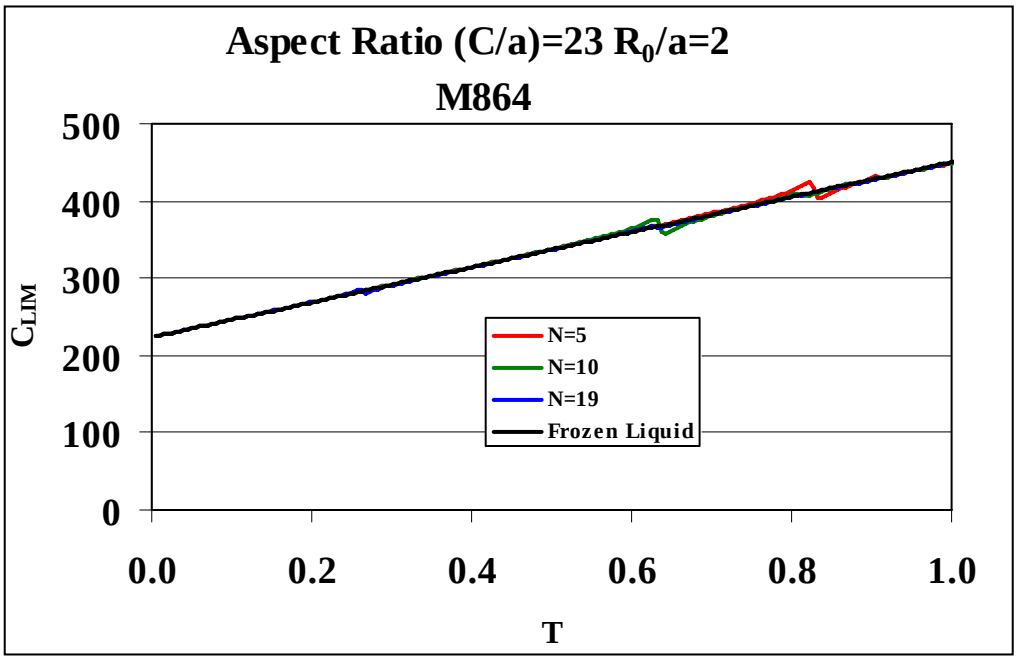

Figure 5. Values of $\mathbf{C_{LIM}}$ showing Eigen frequencies as a function of $\mathbf{T}$ and $\mathbf{N}$.

However, if the parameters and particularly the aspect ratio were to change, instabilities could result. Figure 6 is one such example.

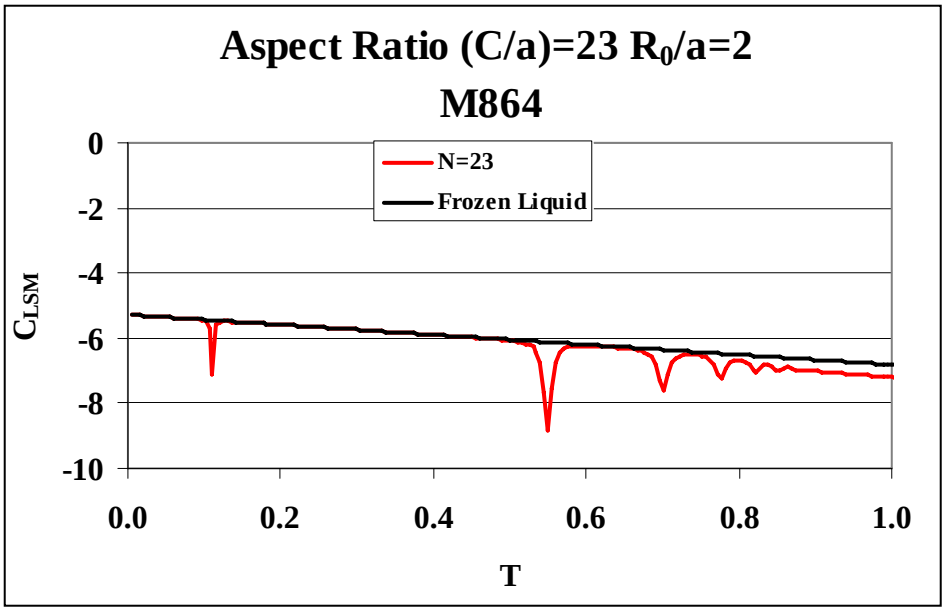

Figure 6. Values of $\mathbf{C_{LSM}}$ showing a possible existence of an instability attributable to an Eigen frequency <0.1.

4. Equations of Motion for the Symmetry Axis Porous Media Configuration

For this problem, the moment arm $R_0 = 0$ so the position vector becomes $\mathbf{R} = (x,\ r\cos\theta,\ r\sin\theta)$ since the candlestick axis is the symmetry axis of the projectile. When the liquid payload axis is coincidental with the projectile symmetry axis, the analysis is simplified if we move to the X', Y', Z' frame rather than the body frame used before. This modifies the transformation given by equation 5 so that

$$\begin{bmatrix} X' \\ Y' \\ Z' \end{bmatrix} = \begin{bmatrix} 1 & 0 & 0 \\ 0 & \cos\left[tPT\right] & -\sin\left[PT\right] \\ 0 & \sin\left[tPT\right] & \cos\left[tPT\right] \end{bmatrix} \begin{bmatrix} 1 & -K_0 e^{\varepsilon TPt} & 0 \\ K_0 e^{\varepsilon TPt} & 1 & 0 \\ 0 & 0 & 1 \end{bmatrix} \begin{bmatrix} 1 & 0 & 0 \\ 0 & \cos\left[tP(T-1)\right] & \sin\left[tPT\right] \\ 0 & -\sin\left[tP(T-1)\right] & \cos\left[tPT\right] \end{bmatrix} \begin{bmatrix} \tilde{X} \\ \tilde{Y} \\ \tilde{Z} \end{bmatrix} \quad (19)$$

and $\tilde{X}, \tilde{Y}, \tilde{Z}$ are coordinates in the non-rolling reference frame. The velocity of the media obtained from the rotation kinematics is now given by

$$
\begin{aligned}
V_r' &= -xK_0 P(S-i)e^{PSt-i\theta} \\
V_\theta' &= P r + ixK0P(S-i)e^{PSt-i\theta} \\
V_x' &= rK_0 P(S-i)e^{PSt-i\theta}
\end{aligned}
\tag{20}
$$

and r, θ, x are cylindrical coordinates in the non-rolling frame. The Euler equations are now modified to account for an inviscid liquid flowing through porous media. This modification assumes that flow in porous media can be represented by additional terms that are proportional to the liquid velocity relative to the media which is taken to be rigidly attached to the coning projectile. Using the factor, $e^{PSt-i\theta}$, for each independent variable allows the modified Euler equations now written in cylindrical components to have the following form:

$$
\begin{aligned}
(S+Ct-i)v - 2w + xCtP(S-i) + \frac{1}{\rho P}\frac{dp}{dr} &= 0 \\
(S+Ct-i)w + 2v - ixC_t P(S-i) - \frac{ip}{\rho P r} &= 0 \\
(S+Cx-i)u \qquad - rC_x P(S-i) + \frac{1}{\rho P}\frac{dp}{dx} &= 0
\end{aligned}
\tag{21}
$$

In this equation, v, w, u are the r, θ, x components of the fluid velocity and p is the perturbation pressure. Note the terms that are proportional to the constants C_t, C_x represent drag that the porous media exerts on flow passing through these media. Motivation for this model stems from Darcy's Law (*12*) which says that the drag force caused by porous media, **Dr**, is given by

$$
\mathbf{Dr} = -\frac{\mu}{\kappa}\mathbf{Vr} = \text{-}\rho P^2 a Cr \frac{\mathbf{Vr}}{P a}
$$

$\mu \rightarrow$ dynamic viscosity

$\kappa \rightarrow$ porosity (dimensions of length (*2*))

$\mathbf{Vr} \rightarrow$ velocity of fluid relative to porous media

$\rho \rightarrow$ liquid density

$\mathbf{Dr} \rightarrow$ pressure gradient induced by the porous media on the fluid flow

$Cr \rightarrow$ dimensionless constant which is a measure of the pressure gradient

so that $Cr = \dfrac{\mu}{\rho \kappa P}$.

Solving equation 21 leads to the velocity field expressions:

$$
\begin{aligned}
v &= -\frac{2ip - \frac{dp}{dr}(S-i)r}{r\rho P(S-3i)(S+i)} - \frac{x C_t P(S-i)}{S + C_t + i} \\
w &= \frac{i(S-i)p + 2r\frac{dp}{dr}}{r\rho P(S-3i)(S+i)} + \frac{i x C_t P(S-i)}{S + C_t + i} \\
u &= -\frac{\frac{dp}{dx}}{\rho P(S-i)} + \frac{r C_x P(S-i)}{S + C_x - i}
\end{aligned}
\tag{22}
$$

Invoking the fact that the flowing liquid is incompressible causes the continuity equation to give the following expression for the perturbation pressure p

$$
\begin{aligned}
r^2\frac{d^2p}{dr^2} + r\frac{dp}{dr} - p - r^2\overline{\sigma}^2\frac{d^2p}{dx^2} &= 0 \\
\overline{\sigma}^2 &= -\frac{(S + C_t - 3i)(S + C_t + i)}{(S + C_t - i)(S + C_x - i)}
\end{aligned}
\tag{23}
$$

Equations 13 and 23 show when $C_t = 0, C_x = 0$ causes $\overline{\sigma}^2 = \sigma^2$. Using the demands of equation 20 modifies the coefficients for the Fourier-Bessel series as follows:

$$
\begin{aligned}
A_j &= \frac{16(-1)^n C S(S-i)(S + C_t - 3i)}{\pi^2 a k^2 N\left(J_1(zz)(S + C_t + i) - zz\, J_0(zz)(S + C_t - i)\right)} \\
zz &= \pi a k\overline{\sigma} N/2C \\
E &= -(S-i)^2 \\
D &= 2C(-N + 2n + 1)(S-i)S/Na \\
F &= 0 \\
\\
0 &\le n \le N
\end{aligned}
\tag{24}
$$

5. Porous Media Liquid Moments

The procedure (equation 16) for calculating liquid side moments gives the following expression for liquid-saturated porous media in N cylinders, separated by impermeable end caps, located along the projectile symmetry axis:

$$T(C_{LSM}+i\,C_{LIM})=\frac{4C^2(S-i)\left((N^2-1)S^2+(C_t+2i)N^2S+(i\,C_t-1)N^2\right)}{3a^2N^2(S+C_t+i)}+$$
$$\frac{-12C^2(S^2-1)-4C^2+3a^2}{12a^2}+\frac{(S-i)^2}{4}+$$
$$-\frac{128C^2S^2(S-i)(S+C_t-3i)}{\pi^4N^2a^2(S+C_t+i)}\sum_{k\in odd}\frac{J_1(zz)}{\left[J_1(zz)(S+C_t+i)-zz\,J_0(zz)(S+C_t-i)\right]k^4} \qquad (25)$$
$$zz\equiv\pi k\bar{\sigma}N/2C$$

Taking the limits of this expression for large N or large C_t gives the frozen limit values of C_{LSM} and C_{LIM} given by (*3*)

$$C_{LSM\_F}=\frac{\varepsilon}{2}\left[1-T\frac{4C^2/a^2+3}{3}\right]$$
$$C_{LIM\_F}=\frac{1}{2}+\frac{4C^2/a^2+3}{12}T(\varepsilon^2-1) \qquad (26)$$

whenever T is not in the neighborhood of an Eigen frequency $S = (i + \varepsilon)T$ which by equation 25 satisfies

$$J_1(zz)(S+C_t+i)-zz\,J_0(zz)(S+C_t-i)=0 \qquad (27)$$

The definition of $\bar{\sigma}$ given in equation 23 shows that the Stewartson tables (*1, 3*) can again be used to find Eigen frequencies, provided that $C_x = C_t$ and S is replaced by $S + C_t$ while these tables are used. In general, these frequencies S will have complex values, $\varepsilon \neq 0$, thus indicating that damping/undamping will occur. The cases when $C_x \neq C_t$ also result in $\varepsilon \neq 0$ but numerical methods need to be used to find such Eigen frequencies.

Scheidegger (*14*) has tabulated permeability's $\kappa \cong 1.0\times10^{-5}\,cm^2$, and assuming that the media studied here for the M864 have similar permeabilities, which average $C_t, C_x \cong 0.6$. Sample plots showing that C_{LSM} and C_{LIM} again approach the values for a frozen liquid as C_t becomes large (see figures 7 and 8), which are in agreement with equation 26 when $\varepsilon = 0$.

Typical plots showing C_{LSM} changing with increasing values of N are given in figure 9. For this plot, the vertical axis assumes values defined as the difference between C_{LSM} and the frozen values given by equation 26:

$$\Delta C_{LSM}\equiv C_{LSM}-C_{LSM\_F} \qquad (28)$$

The sharp peaks indicate Eigen frequencies which are now complex since $C_x = C_t = 1/3$ and therefore $\varepsilon \neq 0$. Evidently, C_{LSM} approaches the values C_{LSM_F} as N gets larger for values of

T sufficiently removed from any Eigen frequencies. In general, such Eigen frequencies are found with a numerical search routine in the complex plane.

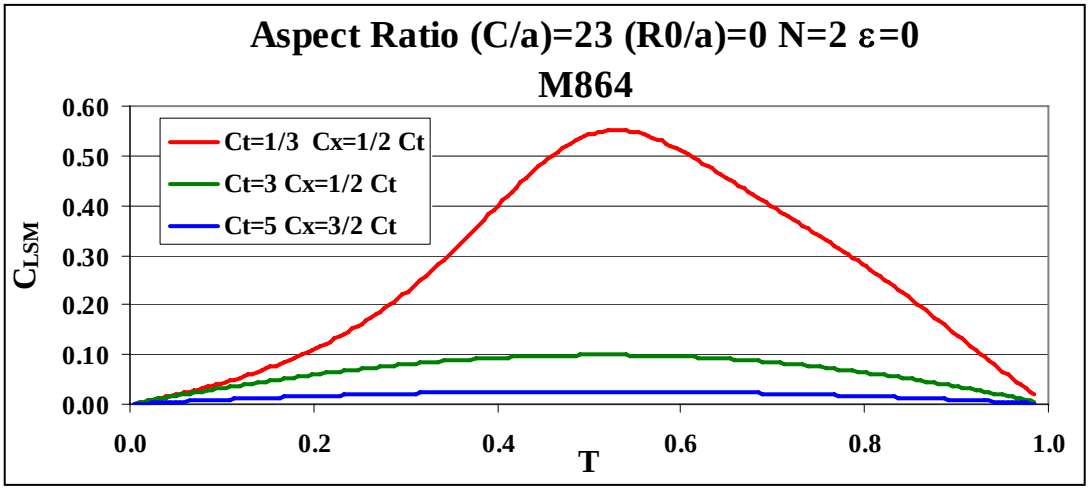

Figure 7. Values of C_{LSM} as a function of T for increasing C_t and C_x.

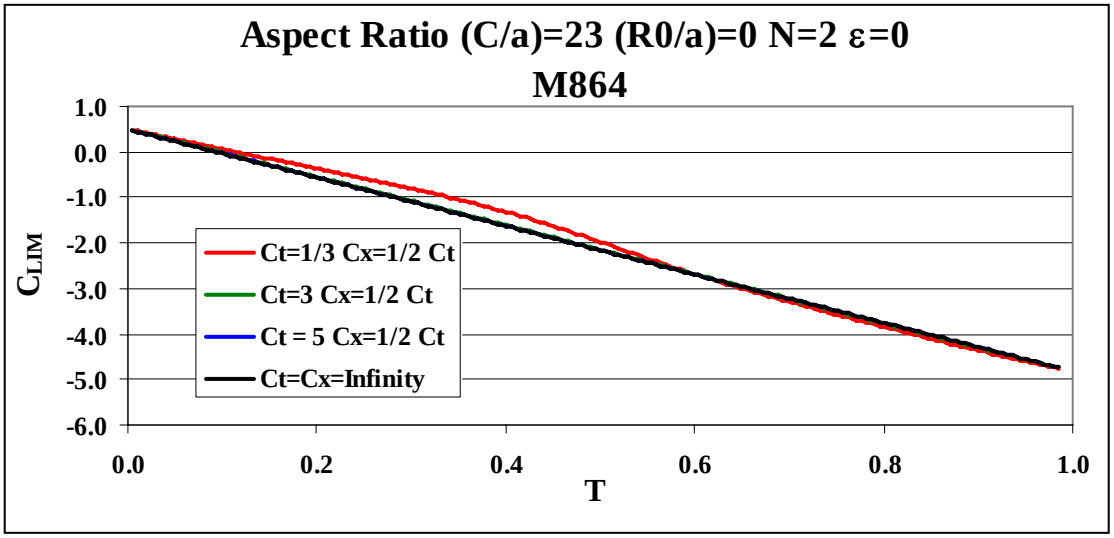

Figure 8. Values of C_{LIM} function of T for increasing C_t and C_x.

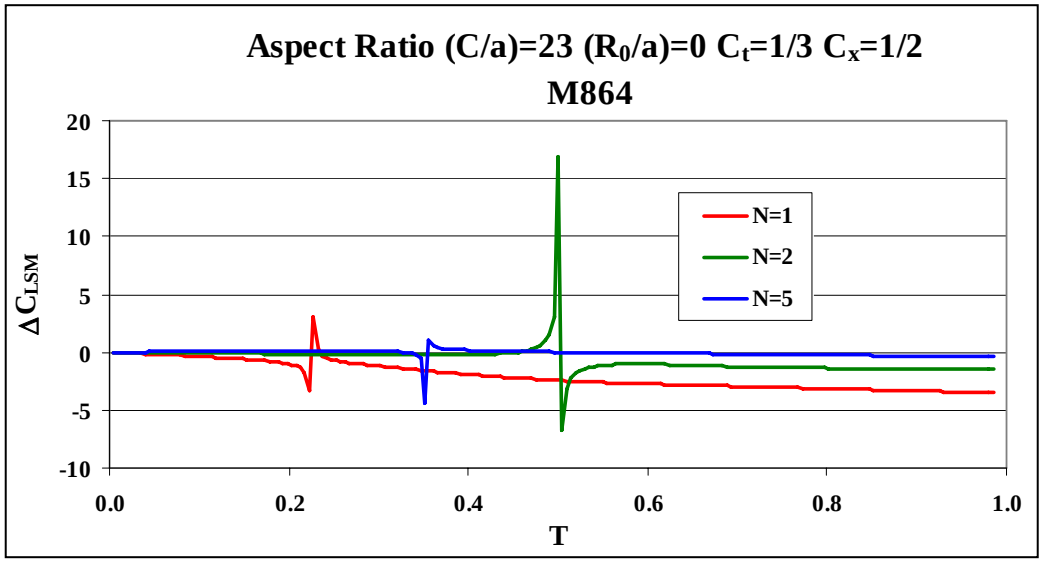

Figure 9. Values of ΔC_{LSM} showing possible flight instabilities (Eigen frequencies) as a function of T. (As N increases, the payload behaves like a frozen [liquid] payload when T is far from Eigen frequencies.)

6. Calculation Method

The equations of the last sections need to be calculated for a wide range of flight, geometry, and porous media parameters all of which require values of Bessel functions. For small values of $|zz|$, simply using power series expansions of each Bessel function works very well. Bessel functions at large values of $|zz|$ were obtained by asymptotic expansions (*13*). Generally, calculating Bessel functions for complex arguments for intermediate values of $|zz|$ is a non-trivial problem and the methods used here employ Gaussian continued fractions. This author has judged that a further discussion of these methods is not appropriate for this article but the reader should be aware of the numerical difficulties associated with calculating complex Bessel functions.

7. Conclusions

The off-axis candlestick problem has been shown to be equivalent to the inviscid Stewartson (*1*) problem whenever porous media are not present or can be ignored. Resonant frequencies are independent of the candlestick off-axis position and can be found with tabulations that have already been found (*1, 3*). Values not found in such tables can readily be obtained by simple numerical root-finding methods. The design configurations examined here show that flight

instabilities should not occur for candlesticks with a low viscosity liquid and as N increases, the liquid behaves more like a frozen liquid.

Cases when the candlestick contains saturated porous media that are located along the symmetry axis of the projectile can possibly force resonances. In these cases, the Eigen S frequencies assume complex values so that damping or un-damping can occur. For the particular case when $C_T = C_X$, it is possible to find the resonances from the Stewartson tables, but if $C_T \neq C_X$, then a numerical search for resonances in the complex plane for the Eigen frequencies is required. The current analysis is based on assumed values of the porosities, C_T C_X, and the results indicate that a flight instability of the M864 is unlikely to transpire. However, if the actual porosity of the proposed media differs significantly from the assumptions used here, catastrophic flight instabilities could result. A thorough search for "problem Eigen frequencies" requires experimental measurements of C_T and C_X in order to gain a better idea where to search, in the complex plane, for such frequencies (*7, 8, 10*). In all cases, the liquid moments approach the values for a frozen liquid with increasing values of N if Eigen frequencies are not present. Similar results also apply for increasing values of C_T.

8. References

1. Stewartson, K. on the Stability of a Spinning Top Containing Liquid. *Journal of Fluid Mechanics* **1959**, *5*, Part 4, 577–592.

2. Wedemeyer, E.H. *Viscous Correction to Stewartson's Stability Criterion*; BRL Report 1325; US Army Ballistic Research Laboratory: Aberdeen Proving Ground, Maryland, June 1966. (AD 489687)

3. Murphy, C.H. *Angular Motion of a Spinning Projectile with a Viscous Liquid Payload*; BRL-MR-3194; U.S. Army Ballistic Research Laboratory: Aberdeen Proving Ground, MD, August 1982. (AD A118676) (See also Journal of Guidance, Control, and Dynamics, Vol. 6. pp.280-286, July –August 1983.)

4. Gerber, N.; Sedney, R. *Moment on a Liquid-Filled Spinning and Nutating Projectile: Solid Body Rotation*; BRL-TR-02470; U.S. Army Ballistic Research Laboratory: Aberdeen Proving Ground, MD, February 1983. (AD A125332)

5. Hall, P.; Sedney, R.; Gerber, N. *Fluid Motion in a Spinning, Coning Cylinder via Spatial Eigen function Expansion*; BRL Technical Report; U.S. Army Ballistic Research Laboratory: Aberdeen Proving Ground, MD, August 1997 (AD A190758)

6. D'Amico, W.P.; Mark, A. *The Application of a Highly Permeable Medium to Reduce Spin-Up Time and to Stabilize a Liquid-Filled Shell*; BRL-MR-02851; U.S. Army Ballistic Research Laboratory: Aberdeen Proving Ground, MD, July 1978. (AD A058595)

7. Miller, M.C.; Molnar, J.W. *Laboratory Studies to Improve Flight Stability of the M825 Projectile*; CRDEC-TR-153; U.S. Army Chemical Research, Development and Engineering Center: Aberdeen Proving Ground, MD, June 1990.

8. Miller, M.C.; Molnar, J.W. *Laboratory Flight Stability Evaluation of M825A1 Production Payloads*; CRDEC-TR-240; US Army Chemical Research, Development and Engineering Center: Aberdeen Proving Ground, MD, October 1990.

9. D'Amico, William P.; Soencksen, Keith P. *Aeroballistic Testing of the M825 Projectile: Phase VII-Larger Radius Felt Wedge Payloads*; ARBRL-MR-3586; US Ballistic Research Laboratory: Aberdeen Proving Ground, Maryland, April 1987.

10. D'Amico, W.P.; Clay, W.H. *Flight Tests for Prototype Felt Wedge/White Phosphorous Improved Smoke Concept*; BRL-MR-02824; U.S. Army Ballistic Research Laboratory: Aberdeen Proving Ground, MD, April 1978. (AD A054643)

11. Cooper, G. R. *Moment Exerted on Coning Projectile by a Spinning Liquid in a Cylindrical Cavity Containing a Porous Medium*; BRL-MR-3677; U.S. Army Ballistic Research Laboratory: Aberdeen Proving Ground, MD, June 1988. (AD A195291)

12. Darcy, H. Les Fontaines Publiques de la Ville de Dijon, 1886.

13. McLachlan, N.W. *Bessel functions for Engineers*; Oxford University Press, London, 1955.

14. Scheidegger, A. E. *The Physics of Flow Through Porous Media*; University of Toronto Press, Canada, 1960.

NO. OF COPIES ORGANIZATION

1 (PDF ONLY) DEFENSE TECHNICAL INFORMATION CTR
DTIC OCA
8725 JOHN J KINGMAN RD
STE 0944
FORT BELVOIR VA 22060-6218

1 US ARMY RSRCH DEV & ENGRG CMD
SYSTEMS OF SYSTEMS INTEGRATION
AMSRD SS T
6000 6TH ST STE 100
FORT BELVOIR VA 22060-5608

1 INST FOR ADVNCD TCHNLGY
THE UNIV OF TEXAS AT AUSTIN
3925 W BRAKER LN STE 400
AUSTIN TX 78759-5316

1 DIRECTOR
US ARMY RESEARCH LAB
IMNE ALC IMS
2800 POWDER MILL RD
ADELPHI MD 20783-1197

1 DIRECTOR
US ARMY RESEARCH LAB
AMSRD ARL CI OK TL
2800 POWDER MILL RD
ADELPHI MD 20783-1197

2 DIRECTOR
US ARMY RESEARCH LAB
AMSRD ARL CI OK T
2800 POWDER MILL RD
ADELPHI MD 20783-1197

1 SCHOOL OF AEROSPACE ENGINEERING
GEORGIA INST OF TECHNOLOGY
ATTN DR M COSTELLO
ATLANTA GA 30332

10 CDR ARDEC
ATTN AMSRD AAR AEM C K CHUNG
R LEE A READDY M CORZO
AMSRD AAR AEM A W KOENIG
B WONG (5 CYS)
PICATINNY ARSENAL NJ 07806-5000

1 MR MILES MILLER
504 HAVERHILL ROAD
JOPPA MD 21085-4319

NO. OF COPIES ORGANIZATION

1 ROY KLINE
27 FREDON GREENDELL RD
NEWTON NJ 07860-5213

ABERDEEN PROVING GROUND

1 DIRECTOR
US ARMY RSCH LABORATORY
ATTN AMSRD ARL CI OK (TECH LIB)
BLDG 4600

2 COMMANDER
US ARMY ECBC
ATTN AMSRD ECB RT D WEBER
BLDG E3516
APG EA

1 DIRECTOR
US ARMY RSCH LABORATORY
ATTN AMSRD ARL WM J SMITH
BLDG 4600

2 DIR USARL
ATTN AMSRD AR WM B M ZOLTOSKI
BLDG 4600

1 DIR USARL
ATTN AMSRD AR WM BA D LYON
BLDG 4600

1 DIR USARL
ATTN AMSRD ARL WM BD B FORCH
BLDG 4600

4 DIR USARL
ATTN AMSRD ARL WM BC P PLOSTINS
G COOPER B GUIDOS
P WEINACHT
BLDG 390

1 DIR USARL
ATTN AMSRD ARL WM BD M NUSCA
BLDG 390